Photochemical and Mutational Analysis of the FMN-Binding Domains of the Plant Blue Light Receptor, Phototropin[†,‡]

Michael Salomon,*[,§] John M. Christie,[||] Elke Knieb,[§] Ulrika Lempert,[§] and Winslow R. Briggs[||]

Botanisches Institut der Universität München, Menzinger Strasse 67, D-80638 München, Germany, and Department of Plant Biology, Carnegie Institution of Washington, 260 Panama Street, Stanford, California 94305

Received March 14, 2000; Revised Manuscript Received May 16, 2000

ABSTRACT: The plant photoreceptor phototropin is an autophosphorylating serine-threonine protein kinase activated by UV-A/blue light. Two domains, LOV1 and LOV2, members of the PAS domain superfamily, mediate light sensing by phototropin. Heterologous expression studies have shown that both domains function as FMN-binding sites. Although three plant blue light photoreceptors, cry1, cry2, and phototropin, have been identified to date, the photochemical reactions underlying photoactivation of these light sensors have not been described so far. Herein, we demonstrate that the LOV domains of *Avena sativa* phototropin undergo a self-contained photocycle characterized by a loss of blue light absorbance in response to light and a spontaneous recovery of the blue light-absorbing form in the dark. Rate constants and quantum efficiencies for the photoreactions indicate that LOV1 exhibits a lower photosensitivity than LOV2. The spectral properties of the photoproduct produced for both LOV domains are unrelated to those found for photoreduced flavins and flavoproteins, but are consistent with those of a flavin−cysteinyl adduct. Flavin−thiol adducts are generally short-lifetime reaction intermediates formed during the flavoprotein-catalyzed reduction of protein disulfides. By site-directed mutagenesis, we have identified several amino acid residues within the putative chromophore binding site of LOV1 and LOV2 that appear to be important for FMN binding and/or the photochemical reactivity. Among those is Cys39, which plays an important role in the photochemical reaction of the LOV domains. Replacement of Cys39 with Ala abolished the photochemical reactions of both LOV domains. We therefore propose that light sensing by the phototropin LOV domains occurs via the formation of a stable adduct between the FMN chromophore and Cys39.

UV-A (320−390 nm) and blue light (390−500 nm) regulate a variety of responses in higher plants. Such processes include phototropism, the inhibition of hypocotyl elongation, stomatal opening, circadian timing, and the expression of specific genes (reviewed in ref *1*). In the past decade, much progress has been made in defining the photoreceptors that mediate the effects of UV-A and blue light in plants. Currently, three plant blue light photoreceptors have been identified: cryptochrome 1 (cry1) (*2*), cryptochrome 2 (cry2) (*3*, *4*), and phototropin 1 (nph1) (*5*). Recent genetic evidence indicates the presence of a fourth blue light receptor, regulating stomatal opening in response to blue light (*6*, *7*).

The third photoreceptor, nph1, functions as a primary photoreceptor for phototropism (*5*, *7*, *8*). Recent studies also indicate an involvement of cry1 and cry2 in the phototropic response (*9*). These findings imply an interaction between the nph1 and cryptochrome signal transduction pathways. The *NPH1* gene has been cloned from several plant species and encodes a blue light photoreceptor that bears no homology to cry1 or cry2. The nph1 protein was therefore named phototropin after its role in phototropism (*1*). The C-terminus of phototropin is very similar to those of serine-threonine protein kinases (*5*). On the other hand, the N-terminal region of the protein contains a repeated motive of 110 amino acids that is related to the well-characterized PAS domains found in a variety of sensor proteins regulated by environmental signals (*10*). PAS domains have been reported to mediate protein−protein interactions, to act as internal sensors of oxygen, redox potential, and light, and to function as cofactor binding sites (*11*). The repeated domains of nph1 are more closely related to a subset of proteins within the PAS domain superfamily that are regulated by either light, oxygen, or voltage. Thus, the PAS domains of phototropin were designated LOV1[1] and LOV2, respectively (*5*).

Heterologous expression studies have recently shown that phototropin noncovalently binds flavin mononucleotide (FMN) as a chromophore and autophosphorylates in response to blue light irradiation (*8*). Moreover, the LOV domains of phototropin were found to bind FMN stoichiometrically when expressed in *Escherichia coli*, demonstrating that both LOV1 and LOV2 function as FMN-binding sites (*12*). The absorption and fluorescence excitation spectra of each of the LOV domains were found to resemble closely the action spectrum

[†] This work was supported by a grant (Ru 108/31-2) of the Deutsche Forschungsgemeinschaft and National Science Foundation Grant IBN901164.

[‡] This is Carnegie Institution of Washington Department of Plant Biology Publication 1444.

* To whom correspondence should be addressed.

[§] Botanisches Institut der Universität München.

[||] Carnegie Institution of Washington.

[1] Abbreviations: FMN, flavin mononucleotide; SDS, sodium dodecyl sulfate; LOV, light, oxygen, or voltage; NPM, *N*-phenylmaleimide.

10.1021/bi000585+ CCC: $19.00
Published on Web 07/11/2000

for phototropism, with fine structure between 400 and 500 nm and a broad peak at 370 nm. Thus, phototropin represents a unique class of flavoprotein photoreceptors, unrelated to the cryptochromes or photolyases.

The LOV domains provide an excellent system for studying the photochemical properties of the blue light receptor phototropin. Attempts to purify phototropin from several plant species have been unsuccessful to date. In contrast, both FMN-binding domains of phototropin can be expressed and purified from *E. coli* in amounts suitable for photochemical characterization (*12*).

In this study, we provide a detailed spectroscopic and biochemical analysis of the LOV1 and LOV2 domains of phototropin. Our findings demonstrate that both of the isolated chromopeptides can function as light sensors under aerobic conditions. In addition, the spectral properties and the results of site-directed mutagenesis indicate that the photochemistry of LOV1 and LOV2 involves the formation of a FMN−thiol adduct with a highly conserved cysteine residue. We therefore believe that the results presented here provide insights into the photochemical reaction mechanism underlying blue light perception by phototropin.

EXPERIMENTAL PROCEDURES

Cloning, Expression, and Purification of the Oat LOV Domains. Cloning of DNA fragments encoding the LOV1 and LOV2 domains from the cDNA of *Avena sativa* nph1 into the bacterial expression vectors pCAL-n and pCAL-n-EK as a fusion to the calmodulin binding peptide (CBP) was carried out as previously described (*12*). The fusion proteins were expressed in either *E. coli* host strain BL21(DE3) or BL21(DE3) pLysS transformed with the recombinant plasmids. Proteins were expressed by adding isopropyl β-D-galactopyranoside (1 mM, final concentration) to cultures at an OD_{600} between 0.2 and 0.3 at 37 °C in ampicillin-containing (50 μg/mL) LB medium. Expression was carried out in darkness for 3.5 h at 30 °C. For cell lysis, the bacteria were frozen overnight at −20 °C in the presence of 0.2% Triton X-100. Purification of the CBP fusion proteins on calmodulin resin was performed according to the instructions from Stratagene. The purified fusion proteins were stored at 4 °C in high-salt elution buffer [1 M NaCl, 50 mM Tris-HCl (pH 8.0), 10 mM β-mercaptoethanol, and 2 mM EGTA].

Site-Directed Mutagenesis of LOV1 and LOV2. Specific mutations were introduced into LOV1 and LOV2 by means of the site-directed mutagenesis method Quick Change (Stratagene). The principle of this method is based on the amplification of the supercoiled double-stranded recombinant plasmid DNA by *Pfu* DNA polymerase using two oligonucleotides, each complementary to opposite strands of the vector and both containing the desired mutation. The parental strands were then digested with *Dpn*I, and the newly synthesized, mutated plasmids were transformed into *E. coli* strain BL21(DE3) or BL21(DE3) pLysS. All single-amino acid exchanges were confirmed by DNA sequencing.

Sequence Alignment and Three-Dimensional Modeling of the LOV Domains. Alignments of the LOV domain sequences of nph1 from *A. sativa*, *Arabidopsis thaliana*, *Oryza sativa*, and *Zea mays*, of npl from *Ar. thaliana*, and phy3 from *Adiantum capillus-veneris* were performed with the program MACBOXSHADE. The three-dimensional structures of LOV1 and LOV2 from *A. sativa* were calculated on the basis of the crystal structure of the PAS domain of the human potassium channel HERG (*27*) with the program Swiss Model (http://www.expasy.ch/swissmod/SWISS-MOD-EL.html). The three-dimensional models were analyzed with the Rasmol and Swiss pdb viewer software.

Light Sources. For light-induced absorbance changes of LOV1 and LOV2, a light source with glass fiber optics and an IR filter (Schott, KL 1500, electronic) was used. UV-A/blue light was generated by a glass filter (filter set for KL 1500, electronic) exhibiting light transmission between 320 and 500 nm with the highest transmission occurring at 400 nm. Blue light (420−500 nm, peak at 450 nm) was obtained by combining the filter described above with a blue glass filter (Schott, BG7) and a cutoff filter (Schott, GG420). The interference filter used to generate monochromatic 445 nm light exhibited a half-bandwidth of 10 nm. Fluence rates were measured with a Li-189 quantum photometer (Lambda Instruments).

Spectroscopy. Ultraviolet and visible absorption spectra and rapid reaction studies of light-induced absorbance changes were assessed with a Transputer Integrated Diode Array Spectrophotometer (TIDAS) and analyzed with the program TISPEC (both from J&M Analytische Mess-und Regeltechnik GmbH). Extinction coefficients of the LOV peptides were determined on the basis of $\epsilon_{445} = 12\,500$ mol^{-1} cm^{-1} for oxidized FMN. Protein concentrations of LOV domain peptides were calculated using the corresponding extinction coefficients.

First-order rate constants for photoproduct formation (k_{ppf}) and dark regeneration (k_{reg}) were calculated using the half-times obtained from the linear semilogarithmic plots shown in Figure 3. Thus, the equilibrium constant (K_{eq}) is represented by k_{ppf}/k_{reg}. Approximate quantum efficiencies (ϕ) were calculated from the equation $\phi = C/Ixa$, where C is the amount of product formed in nmol^{-1} s^{-1}, I is the fluence rate in nmol s^{-1}, and a is the fraction of excitation light absorbed by the sample. I was approximately corrected for the concentration of the unreacted pigment.

Fluorescence excitation spectra between 300 and 500 nm were recorded at room temperature with a Hitachi fluorimeter F-2000 with a band-pass of 10 nm. Integration times of 0.05, 0.25, and 1 s were used, resulting in total scan times of 10 (1200 nm/min), 50 (240 nm/min), and 200 s (60 nm/min). The emission wavelength was 520 nm in each case. Circular dichroism (CD) spectra in the 260−500 nm spectral region were recorded at 2 °C on an Instruments SA/Jobin Yvon CD6 instrument using quartz cuvettes with a 10 mm light path. For CD measurements, proteins were dissolved in 100 mM NaCl and 50 mM Tris-HCl (pH 8.0) and their solutions adjusted to an OD_{445} of 0.6, corresponding to a protein concentration of approximately 50 μM.

Treatment of LOV Domain Fusion Proteins with N-Phenylmaleimide (NPM). To study the effects of NPM on FMN binding, 400 μL of purified LOV domain fusion proteins (1−5 μM) in high-salt elution buffer without β-mercaptoethanol was divided into two identical aliquots. One sample was supplied with 2 μL of 1 M NPM dissolved in dimethyl sulfoxide (DMSO) and the other with 2 μL of pure DMSO. Both samples were incubated for 60 min at room temperature. Samples were mixed with 300 μL of a saturated ammonium sulfate solution, placed on ice for 30

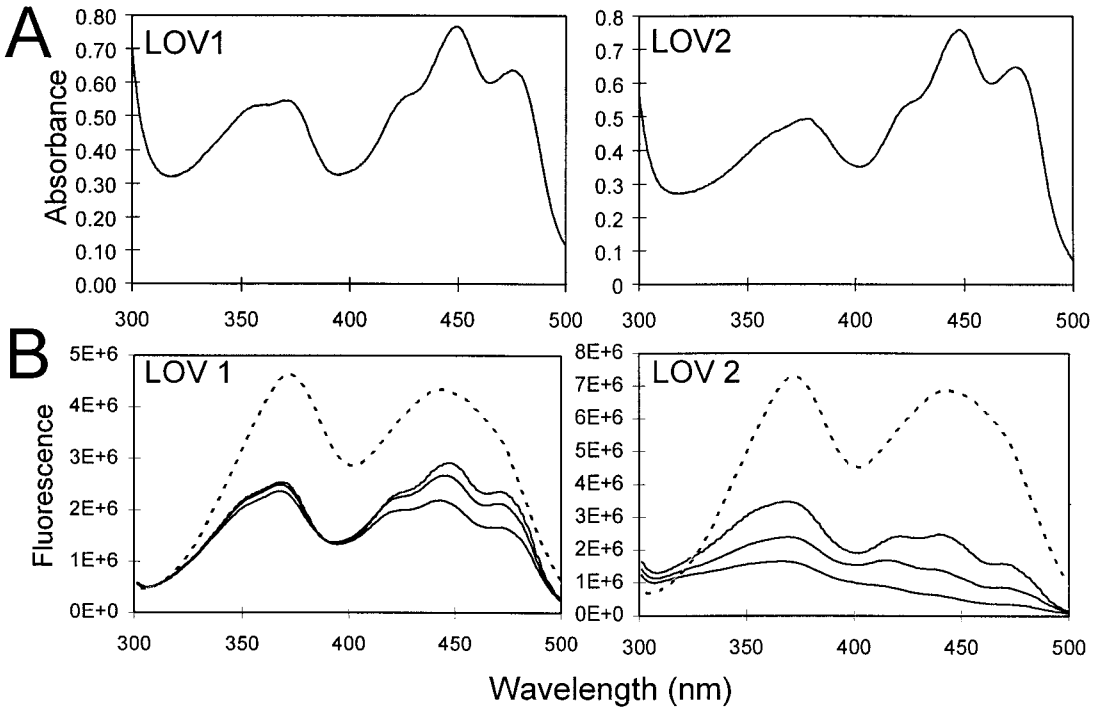

FIGURE 1: Spectral properties of the phototropin LOV domains. (A) Absorption spectra of LOV1 (left panel) and LOV2 (right panel). Peptide concentrations were 61 and 54 μM, respectively. (B) Effect of increasing excitation intensities on the fluorescence excitation spectra of LOV1 (1.4 μM protein) (left panel) and LOV2 (2.2 μM protein) (right panel). Excitation spectra of LOV1 and LOV2 (solid lines) were recorded at scan velocities of 1200 (top line), 240 (middle line), and 60 nm/min (bottom line), resulting in total scan times of 10, 50, and 200 s, respectively ($\lambda_{em} = 520$ nm). The relative degree of fluorescence quenching of the bound FMN chromophore by its protein environment of LOV1 and LOV2 was determined by comparing the fluorescence excitation spectrum of native LOV domains with that of the chromophore released by SDS denaturation (dashed lines, scan velocity of 1200 nm/min).

min, and microcentrifuged at 4 °C for 20 min. The supernatant was removed and the precipitated protein dissolved in 500 μL of high-salt elution buffer (without β-mercaptoethanol). For both fractions, fluorescence excitation spectra (300−500 nm) were recorded. The fraction of FMN specifically released from the flavoprotein in response to the NPM treatment was calculated by comparing the fluorescence intensities found in the supernatant and protein fractions relative to those determined for the control reactions.

RESULTS

Spectroscopic Analysis of LOV1 and LOV2. A detailed spectroscopic analysis of the LOV1 and LOV2 domains of oat phototropin shows substantial differences between the two chromophore binding domains. The LOV domains were found to differ in regard to their respective absorption spectra, fluorescence characteristics, and light-induced spectral changes. The absorption spectra of LOV1 and LOV2 are shown in Figure 1A. Although the absorption spectra of LOV1 and LOV2 are very similar, they are not identical. First, the absorption spectrum of LOV1 has a double-peak structure at 361 and 370 nm, while the component at 361 nm is reduced to a minor shoulder in the absorption spectrum of LOV2, with the major UV-A absorption maximum occurring at 378 nm. Second, the absorption maximum in the blue region of the spectrum is at 449 nm for LOV1 and 447 nm for LOV2. Finally, maximum absorption in the UV-A is greater in LOV1 than in LOV2. The spectral differences mentioned above in light absorption are also reflected by the different extinction coefficients determined for LOV1 ($\epsilon_{449} = 12\,200$ mol^{-1} cm^{-1}, $\epsilon_{370} = 10\,000$ mol^{-1} cm^{-1}) and LOV2 ($\epsilon_{447} = 13\,800$ mol^{-1} cm^{-1}, $\epsilon_{378} = 8700$ mol^{-1} cm^{-1}).

Further differences between the two flavoproteins were observed by fluorescence spectroscopy. With higher excitation intensities or longer scan times, both LOV1 and LOV2 fusion proteins exhibited decreased fluorescence, with the response more pronounced for LOV2 than for LOV1 (Figure 1B). We determined the relative amounts of fluorescence loss by comparing the fluorescence of the peptide-bound FMN (solid lines) with that of the FMN released following SDS denaturation of the holopepetides (dashed line). At a scan speed of 1200 nm/min (top solid lines), the ratios of free versus bound FMN for excitation wavelengths of 370 and 445 nm are 1.79 and 1.45 for LOV1 and 2.05 and 2.75 for LOV2, respectively. Fluorescence loss for the FMN chromophore therefore appears to be significantly greater for LOV2 than for LOV1 (Figure 1B).

The light-inducible fluorescence changes were fully reversible in the dark, indicating that there was no permanent photodamage of the LOV domains and that both fusion peptides were capable of undergoing some kind of photocycle. Because light treatment appeared to cause a photobleaching reaction, we next investigated the light-inducible effects on the absorption spectra of LOV1 and LOV2.

Reversible Photobleaching of LOV1 and LOV2. To determine whether the light-mediated loss in fluorescence observed for LOV1 and LOV2 corresponds to specific absorbance changes, we performed time-resolved UV−visible spectrophotometry. Light-induced absorbance changes were detected for both LOV domains of phototropin in response to exposure to high-intensity white light (45 000

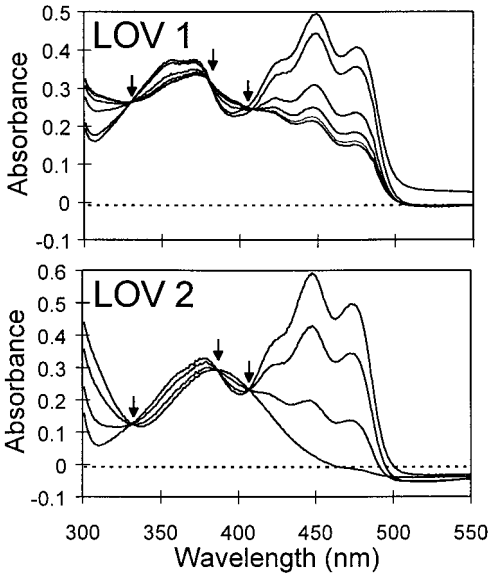

FIGURE 2: Reversible photobleaching of LOV1 and LOV2. Absorbance changes measured for LOV1 (top panel) and LOV2 (bottom panel) on exposure to high-intensity white light (45 000 μmol m^{-2} s^{-1}). The uppermost curves in each panel represent the initial dark spectra recorded for LOV1 and LOV2. After the onset of illumination, spectra were recorded at 2 s intervals for LOV1 and 0.7 s intervals for LOV2. The isosbestic points located at 331, 385, and 407 nm are indicated by arrows.

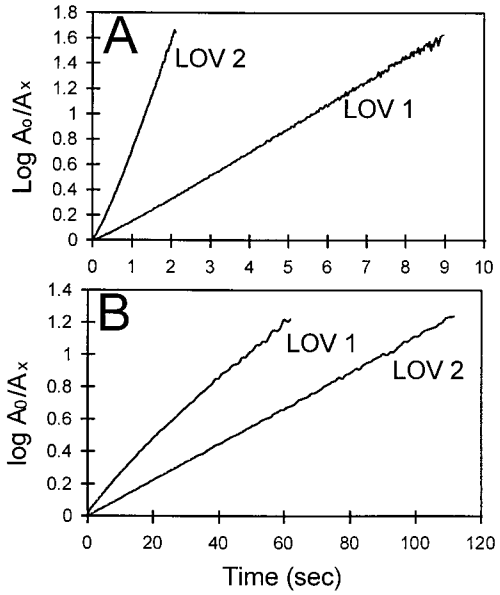

FIGURE 3: Reaction kinetics for photoproduct formation (A) and dark regeneration (B) for LOV1 and LOV2. Kinetics of photoproduct formation were monitored on ice, whereas the kinetics of dark regeneration were recorded at room temperature. The kinetic data were obtained by following the absorbance changes at 449 nm for LOV1 and at 447 nm for LOV2. Spectra were recorded at intervals of 32 ms (A) or 1.05 s (B). A_0 represents the amount of unreacted flavoprotein (A) or photoproduct (B) at time zero. A_x represents the corresponding amount of unreacted flavoprotein (A) or photoproduct (B) at time *x*.

μmol m^{-2} s^{-1}) (Figure 2). The geometry was such that the entire sample was illuminated to avoid problems arising from pigment molecules diffusing into and out of the light beam. In each case, irradiation resulted in a rapid loss of absorbance in the blue region of the spectrum and the concomitant appearance of an absorption band at 380 nm. However, for LOV1 the maximum difference in absorption at 449 nm between the nonirradiated and irradiated species was only 60% of the value obtained for LOV2 at 447 nm. In agreement with the results of the fluorescence studies described above, the light-driven reaction was fully reversible and the blue light-absorbing form of the proteins was fully restored after the external light source was switched off. These findings therefore demonstrate that the LOV domains of phototropin exhibit a light-sensing function and undergo a photocycle. In each case, the LOV domains of phototropin were remarkably stable since each sample could be photobleached more than 20 times without any measurable loss in light responsiveness or alteration of the absorption spectrum.

To quantitate the kinetics of photoproduct formation and regeneration, the absorbance changes at 449 nm for LOV1 and 447 nm for LOV2 were followed. For both processes, semilogarithmic plots of photoproduct formation or dark regeneration of the blue light-absorbing form versus time were linear, indicating that these reactions are all first-order (Figure 3). The half-times for the dark reaction at room temperature are 11.5 s for LOV1 and 27 s for LOV2, resulting in corresponding regeneration rate constants (k_{reg}) of 6×10^{-2} and 2.55×10^{-2} s^{-1}, respectively. When dark regeneration was carried out on ice, a 7-fold slower rate was measured for both proteins, giving k_{reg} values of 8.9×10^{-3} (LOV1) and 3.4×10^{-3} s^{-1} (LOV2), while the rates of photobleaching remained unchanged (Table 1). Since the chemical equilibrium at the lowered temperature favors photoproduct formation by a factor of 7, the kinetics of

Table 1: Differential Light Sensitivity of LOV1 and LOV2[a]

	LOV1	LOV2
light source	WL, UV-A/BL, BL, 445 nm	WL, UV-A/BL, BL, 445 nm
intensity (μmol m^{-2} s^{-1})	45 000, 3000, 110, 55	45 000, 3000, 110, 55
protein concentration (μM)	39.7, 38.6, 32.5, 32.5	41.3, 70.3, 33.3, 51.6
k_{ppf}, room temp (s^{-1})	0.364, nd, nd	1.44, nd, nd, nd
k_{ppf}, ice (s^{-1})	0.364, 0.09, 0.01	1.44, 0.92, 0.106, 0.058
k_{reg}, room temp (s^{-1})	0.06, −, −, −	0.0255, −, −, −
k_{reg}, ice (s^{-1})	0.0089, −, −, −	0.0034, −, −, −
k_{eq} (=k_{ppf}/k_{reg}), ice	41, 10.1, 1.12	423, 270, 31, 17
% photoproduct, ice	60, 52, 10, 0	100, 100, 95, 97
quantum efficiency	nd, nd, 0.045	nd, nd, 0.44, nd

[a] k_{ppf} and k_{reg} are the rate constants for photoproduct formation and regeneration, respectively. k_{eq} is the equilibrium constant (k_{ppf}/k_{reg}). WL is white light, BL blue light, and nd nondetermined.

LOV1 and LOV2 photobleaching were studied on ice. As shown in Table 1, the light-induced bleaching of LOV1 and LOV2 exhibits a strict dependence on both the light quality and the fluence rate that is used.

Given the rate constants and other parameters shown in Table 1, and the approximate log linearity of the photobleaching reaction (Figure 3), relative quantum efficiencies for the photoreactions were calculated using the data obtained with the broad-band blue light source (Table 1). The values were 0.045 for LOV1 and 0.44 for LOV2. Hence, the considerably lower extent of photobleaching of LOV1

compared to that of LOV2 (Figure 2), under conditions resulting in an equilibrium between the light and dark reactions, illustrates two major difference between the LOV domains. First, the dark regeneration rate for LOV1 is more than twice that for LOV2. Second, the relative quantum efficiency for the photobleaching reaction of LOV1 is $^1/_{10}$ of that for LOV2.

Differential Dark−Light Absorption Spectra of LOV1 and LOV2 Suggest the Formation of a Flavin−Thiol Adduct. In general, photobleaching of flavins and flavoproteins is a consequence of photoreduction. The reaction is typically carried out anaerobically under high-intensity light conditions in the presence of an electron donor such as EDTA and involves the light-driven reversible reduction of the isoalloxazine ring system. The flavin is reduced either directly to its two-electron reduced form or via a one-electron-reduced state or semiquinone. The kinetics of photoreduction for most flavoproteins are generally 2−3 orders of magnitude slower than those of free flavins, the latter usually occurring within a matter of seconds (*13*). The spectra recorded during the chemical reduction or photoreduction of flavins are characterized by a loss in absorbance in both the UV-A and blue light regions of the spectrum, with a single isosbestic point occurring between 330 and 350 nm (*14*, *15*).

The characteristics of the light-induced absorbance changes detected for both LOV domains of phototropin are not consistent with typical flavin reductions. First, the above spectral changes for LOV1 and LOV2 are detected under aerobic conditions. Preliminary analysis indicates that both photobleaching and dark regeneration of the phototropin LOV domains occur under anaerobic conditions (data not shown), indicating that oxygen is not essential for either reaction. However, detailed kinetics for the forward and reverse reactions under anaerobic conditions have not yet been obtained. Second, the kinetics of photoproduct formation for both LOV domains with high-intensity white light are very rapid, occurring within a few seconds (Figure 2). In each case, the absorption maximum in the UV-A shows a shift of 8 nm to the blue,[2] whereas the overall amount of UV-A absorption is only slightly reduced. Third, the differential dark−light absorption spectra of LOV1 and LOV2 exhibit three isosbestic points between 300 and 500 nm (331, 385, and 408 nm, Figure 2, arrows). Hence, the reaction mechanism underlying phototropin photoactivation is quite unlike that of the typical redox-catalyzed reduction of other flavoproteins.

To our knowledge, the only spectra that exhibit spectral characteristics similar to those found for LOV1 and LOV2 are those measured for the formation of flavin C(4a)−thiol adducts. Thiol adducts are generally short-lifetime reaction intermediates and have been described for flavoproteins with redox-active disulfides such as mercuric ion reductase (*16*), lipoamide dehydrogenase (*17*, *18*), and thioredoxin reductase (*19*). By site-directed mutagenesis, Miller et al. (*16*) succeeded in trapping the thiol intermediate of mercuric ion reductase in a sufficiently stable form to obtain its absorption spectrum. (see Figure 3 in ref *16*). The spectral changes obtained for the mutated enzyme during the formation of the C(4a)−cysteinyl adduct are very similar to those found for the light-induced spectral changes of the LOV domains: a strong decay in blue light absorption with a shift of the UV-A absorption maximum to longer wavelengths resulting in three isosbestic points at 330, 375, and 410 nm. Thus, the photochemical reactions observed for the LOV1 and LOV2 domains of phototropin suggest that the reaction mechanism involves the formation of a similar flavin−thiol adduct.

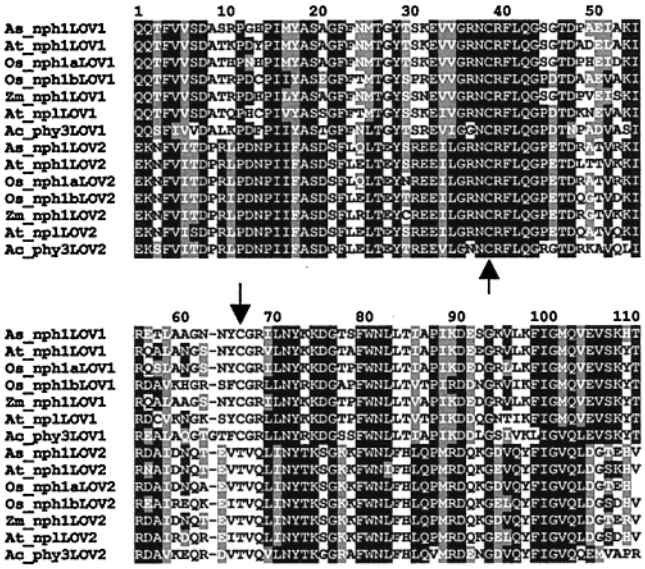

FIGURE 4: Sequence alignment of the LOV domains from higher-plant phototropin and phototropin-like proteins: phototropin from *A. sativa* phototropin (As_nph1LOV1 and As_nph1LOV2), *Ar. thaliana* phototropin (At_nph1LOV1 and At_nph1LOV2), *Z. mays* (Zm_nph1LOV1 and Zm_nph1LOV2), and *O. sativa* (Os_nph1aLOV1, Os_nph1aLOV2, Os_nph1bLOV1, and Os_nph1bLOV2). Also shown are the LOV domains from *Ar. thaliana* npl1 (At_nplLOV1 and At_nplLOV2) and *Ad. capillus-veneris* phy3 (Ac_phy3LOV1 and Ac_phy3LOV2). Arrows indicate the position of Cys39 within the conserved region GRNCRFLQG of LOV1 and LOV2, and the position of Cys66 in LOV1. Identical amino acids are shaded in black, and similar amino acids are shaded in gray.

Three-Dimensional Modeling of LOV1 and LOV2. Formation of a flavin−thiol adduct requires the presence of at least one cysteine in proximity to the flavin chromophore. Alignment of the LOV domains from oat (*20*), *Arabidopsis* (*5*), maize, and rice phototropins (GenBank accession numbers AF033263, AB0108443, and AB0108444), *Adiantum* phy3 (*21*), and *Arabidopsis* npl (*22*) (Figure 4) shows that both LOV domains contain a conserved cysteine residue (Cys39). To simplify the numbering system, we refer to the amino acid positions located within the actual 110-amino acid stretch of the LOV domains and not to the relative positions within the full-length protein. Unlike LOV2, the LOV1 domain contains a second cysteine at position 66 (Cys66) (Figure 4). Residue Cys39 is part of the motif GRNCRFLQG, a conserved region found in all LOV domains of phototropin and phototropin-like proteins identified to date (the first R is not conserved in the LOV domains of phy3). Therefore, Cys39 is a likely candidate for the formation of a cysteinyl adduct with the protein-bound FMN chromophore.

To obtain additional structural information about the phototropin LOV domains, we performed computer-based three-dimensional modeling (*23*−*25*). The crystal structures

[2] In photobiology, a blue shift usually means a shift toward shorter wavelengths and a red shift a shift toward longer wavelengths. Thus, the expression used here may lead to some confusion.

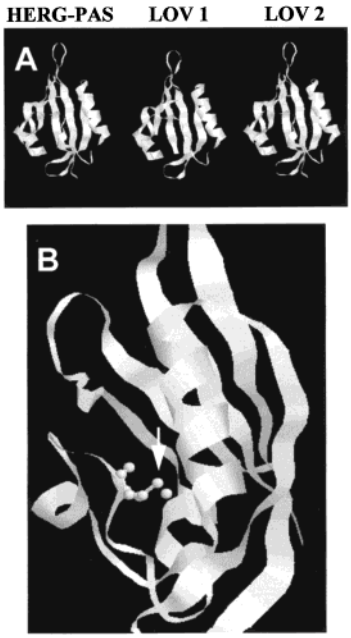

FIGURE 5: Computer-based three-dimensional models of LOV1 and LOV2 from oat phototropin. (A) The structures of LOV1 and LOV2 were calculated using the crystal structure of the PAS domain from the human potassium channel protein, HERG (HERG-PAS). The five antiparallel β-sheets and the two α-helices of HERG-PAS and the predicted LOV domain models are shown. (B) Position of residue Cys39 within the central PAS core of the predicted three-dimensional model of LOV2. The model is turned 90° to the left with respect to its position in panel A. The arrow indicates the position of the sulfur atom of Cys39.

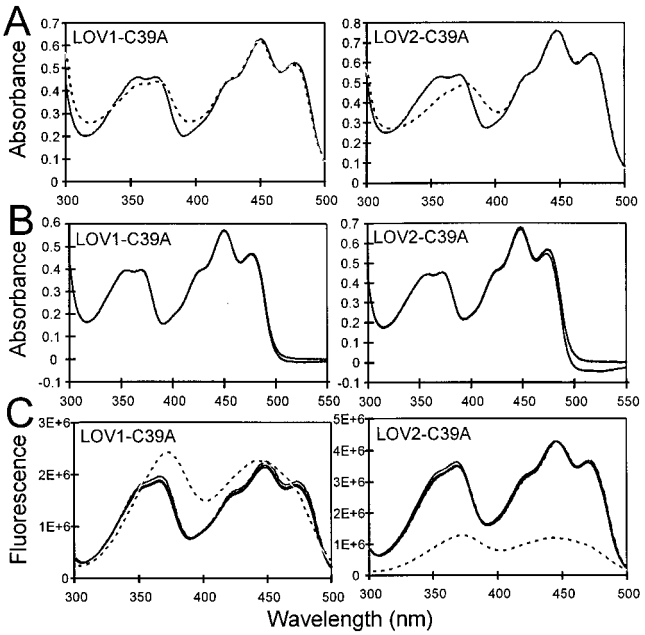

FIGURE 6: Spectral properties of the LOV1C39A and LOV2C39A mutant proteins. (A) Absorption spectra of LOV1C39A (50 μM) and LOV2C39A (55 μM) mutant proteins (solid lines) relative to that of the native LOV domain proteins (dashed lines). (B) For both mutant proteins, the absorption spectra remained unchanged upon irradiation with high-intensity white light (45 000 μmol m^{-2} s^{-1}). Spectra recorded prior to irradiation and 5, 10, and 15 s after the light source was switched on are shown. Peptide concentrations were 47 μM for LOV1C39A and 49 μM for LOV2C39A. (C) Fluorescence excitation spectra (solid lines) obtained for LOV1C39A (0.8 μM) (left panel) and LOV2C39A (0.35 μM) (right panel) at increasing total scan times (10, 50, and 200 s) and fluorescence excitation spectrum of FMN released from LOV1C39A and LOV2C39A (dashed lines) (for details, see Figure 1). λ_{em} = 520 nm.

of three PAS domains have recently been determined (*26*−*28*). The PAS domain from the human potassium channel protein, HERG (HERG-PAS) (*27*), was used as a structural template for modeling of the oat LOV domains since the sequence of HERG-PAS is approximately 30% identical to those of LOV1 and LOV2. As depicted in Figure 5A, the predicted three-dimensional structures of LOV1 and LOV2 are very similar to that of HERG-PAS, containing five β-sheets and two α-helices as their basic secondary structure elements. The predicted models of LOV1 and LOV2 suggest that the side chain of Cys39 is buried deep within the molecule (Figure 5B), in proximity (4.5 Å) to the hydrophobic side chains of amino acids Val5, Phe23, Phe41, and Leu42 in LOV1 and Phe23, Ile34, Phe41, and Leu42 in LOV2. Hence, on the basis of the modeling analysis, residue Cys39 appears to be embedded in a hydrophobic core for both LOV1 and LOV2. Hydrophilic residues in each of the LOV domain models are also positioned within 4.5 Å of Cys39. These are Asn38, Arg40, Gln43, Asn71, and Gln102. However, in each case, these side chains are predominantly oriented toward the outer surface of the molecule.

Spectroscopic Analysis of LOV Domain Cys39 Mutants. On the basis of the predicted three-dimensional structures, we investigated whether Cys39 of LOV1 and LOV2 might play a role in the formation of the postulated light-induced flavin−cysteinyl adduct. We introduced mutations at this position for both LOV1 and LOV2 and examined their effects on FMN binding and/or the spectral properties. In each case, the LOV1C39A and LOV2C39A mutant proteins that were generated were unaffected in their capacity to bind FMN relative to the native proteins. However, the spectral properties of the mutant flavoproteins were found to differ somewhat from those of their wild-type counterparts (compare the dashed and solid lines in Figure 6A). LOV2C39A displays a somewhat altered absorption spectrum that is similar to that of the wild-type LOV1 domain, exhibiting a higher level of absorbance in the UV-A region with absorption peaks at 356 and 372 nm (Figure 6A).

The most striking difference between the C39A mutant proteins and the wild-type LOV domains is that neither LOV1C39A nor LOV2C39A undergoes the light-induced spectral changes characteristic of LOV1 and LOV2. For both mutant chromopeptides, illumination with high-intensity white light did not affect the absorption spectrum; no light-mediated photobleaching was detected for these proteins (Figure 6B). Similarly, the fluorescence excitation spectra for both C39A mutants retained their shape independent of whether the spectra were recorded at a scan velocity of 1200, 240, or 60 nm/min (Figure 6C). Thus, replacement of residue Cys39 with Ala results in a loss of the photochemical reactions typically observed for LOV1 and LOV2 under identical conditions (see Figures 1B and 2).

Both C39A mutant apoproteins exhibited less fluorescence quenching of the bound FMN chromophore by its protein environment. For LOV1C39A, the FMN fluorescence of the holoprotein was approximately equal to that of the free chromophore released by SDS denaturation (Figure 6C). For LOV2C39A, the fluorescence of the protein-bound FMN was found to be 4-fold higher than the fluorescence measured

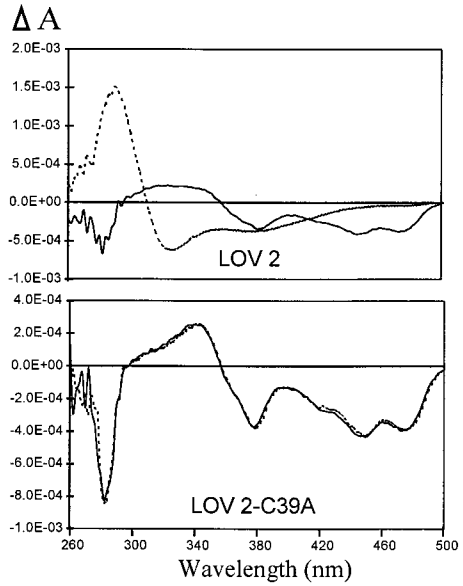

FIGURE 7: Circular dichroism spectra of LOV2 and LOV2C39A in the near-ultraviolet to visible spectral region (260−500 nm) in the dark (solid curves) and after irradiation for 5 s with white light (45 000 μmol m^{-2} s^{-1}) (dashed curves). All spectra represent the means of eight individual measurements and were measured in a 10 mm quartz cuvette. The light samples were irradiated prior to each measurement. The concentrations of LOV2 and LOV2C39A were 48 and 52 μM in 100 mM NaCl and 50 mM Tris-HCl (pH 8.0), respectively. To slow the regeneration process and to stabilize the light-induced spectral changes, measurements were carried out at 2 °C.

for the released chromophore (Figure 6C). These findings indicate that residue Cys39 is essential for LOV1 and LOV2 photobleaching and provide evidence that the photobleaching reaction occurs via the formation of a FMN−cysteinyl adduct.

Light-Induced Circular Dichroism Changes. To establish whether the chromophore of the recombinant phototropin LOV domains undergoes a conformational change upon irradiation, we recorded circular dichroism (CD) spectra in the near-UV to visible region of flavin absorption (260−500 nm) under dark and light conditions. Nonirradiated samples of LOV2 exhibited strong negative absorption bands near 275, 380, 450, and 475 nm and a weak positive band in the 310−350 nm region of the spectrum (Figure 7). The CD spectrum for LOV2 changed dramatically when the sample was illuminated prior to measurement. As shown in Figure 7, the negative band at 275 nm is completely reversed and shifted by 10 nm toward longer wavelengths. The opposite effect occurs for the broad positive band at 310−350 nm. The minor changes observed in the visible range (350−500 nm) are likely to reflect the light-induced loss of blue light absorbance characteristic of LOV2 rather than a reduced absorption of the negatively polarized light beam. These observations strongly suggest that the chromophore of LOV2 undergoes a conformational change(s) in response to illumination.

We then examined whether these properties were altered in the C39A mutant of LOV2. In the case of LOV2C39A, the CD spectrum of the nonirradiated chromoprotein is similar to that of the native (Figure 7). However, no changes in the CD spectrum of the C39A mutant protein were observed in response to high-intensity white light treatment.

Table 2: Effects of Single-Amino Acid Exchanges on FMN Binding and Photochemical Reactivity of LOV1 and LOV2

	% reduced FMN binding	photochemical reactivity
LOV1S20F	>98	no chromophore
LOV1F23Y	>98	no chromophore
LOV1N38D	95	not measurable
LOV1C39A	0	blocked
LOV1R40D	>98	no chromophore
LOV1C66S	30	slightly enhanced
LOV2S20F	>98	no chromophore
LOV2F23Y	70	reduced
LOV2N38D	80	reduced
LOV2C39A	0	blocked
LOV2R40D	>98	no chromophore
LOV2Q43H	60	reduced

These data indicate that Cys39 is directly involved in the production of a conformational change of the FMN chromophore.

The CD spectrum of LOV1 differs from that of LOV2 in that the negative 275 nm peak is less prominent (data not shown). The spectrum for LOV1 also exhibits an additional strong positive band at 265 nm. Since LOV1 protein preparations routinely contained a higher degree of contaminating *E. coli* proteins than those of LOV2, we cannot exclude the possibility that the additional 265 nm peak is derived from impurities within the sample. Nevertheless, similar light-induced CD changes were observed for native LOV1. These changes were not as dramatic as those found for LOV2, most likely because of the reduced photosensitivity of this domain and hence the lower photoproduct yields (see Figure 2). Nevertheless, as for LOV2, these changes were undetectable in the LOV1C39A mutant (data not shown).

Effects of Other Amino Acid Substitutions. In addition to the C39A mutations, we also studied the effects of other single-amino acid exchanges on the function of LOV1 and LOV2. To minimize introducing mutations that may have an adverse effect on protein structure, amino acids were replaced by conservative substitutions or by corresponding amino acid side chains found in PAS domains from other proteins. On the basis of the predicted three-dimensional models of LOV1 and LOV2, the majority of the amino acid residues selected for in vitro mutagenesis were in proximity to Cys39. The only exceptions were the exchanges of Cys66 with Ser in LOV1 (LOV1C66S) and Ser20 with Phe in LOV1 and LOV2 (LOV1S20F and LOV2S20F, respectively). The S20F exchange corresponds to a point mutation found in the LOV domain of the putative blue light photoreceptor, white collar-1 (WC-1) from *Neurospora crassa* that eliminates blue light sensitivity in this organism (*29*).

As summarized in Table 2, all of the additional amino acid substitutions resulted either in complete loss of FMN binding, as in the case of S20F (LOV1S20F and LOV2S20F) and R40D (LOV1R40D and LOV2R40D), or in different levels of reduced chromophore binding. The latter is valid for the amino acid exchanges F23Y and N38D for both LOV domains, C66S for LOV1 and Q43H for LOV2. Interestingly, LOV1 appeared to be more sensitive to such changes than LOV2. In addition to a reduced level of FMN binding, LOV2F23Y, LOV2N38D, and LOV2Q43H also exhibited a reduced photochemical reactivity compared to the wild-

Table 3: Effects of NPM on FMN Binding for LOV1, LOV2, and Mutated LOV Proteins[a]

	% bound FMN	% released FMN
LOV1	15	85
LOV1C66S	16	84
LOV1C39A	90	10
LOV2	100	0
LOV2C39A	100	0
LOV2Q43H	20	80

[a] The values shown give the relative fluorescence of protein-bound vs FMN released from the different flavoproteins after incubation in the presence of 10 mM NPM for 60 min at room temperature in comparison to those found in control reactions without NPM.

type protein (Table 2). In fact, the spectral characteristics of these mutants resemble those of the LOV1 domain where irradiation results in photoproduct accumulation at steady state rather than those of LOV2. However, further interpretation of these results would be premature in the absence of a detailed structure for the LOV domains obtained by X-ray crystallography.

Reaction of Cys39 with N-Phenylmaleimide (NPM). Further structural information about the FMN-binding sites of LOV1 and LOV2 were provided by studies with the sulfhydryl group alkylating reagent NPM. We investigated its effect on both LOV domains at concentrations ranging from 0.1 to 10 mM. At protein concentrations of 1−5 μM, incubation of LOV1 in the presence of a large excess of NPM (10 mM) led to the release of the FMN chromophore (85%) within 1 h at room temperature (Table 3). In comparison to the native protein, the fluorescence excitation spectrum of the released chromphore is characteristic of free flavins with no degree of fine structure in the blue region of the spectrum. By contrast, NPM had no effect on LOV2 or the LOV2C39A mutant, even after several hours. This result is consistent with the predicted three-dimensional models obtained for the phototropin LOV domains, which show that Cys39 of LOV1 is more accessible to the outside environment than Cys39 of LOV2.

To determine which of the cysteine residues found in LOV1 react with NPM to result in a release of the chromophore from the FMN-binding site, we examined the effects of NPM on the LOV1 mutants, C66S and C39A. Replacement of Cys66 with Ser did not prevent the NPM-mediated release of FMN from the holoprotein. However, for the C39A mutation more than 90% of the chromophore was retained after treatment for 1 h with NPM. Hence, the site of NPM modification is likely the SH group of Cys39 as when Cys39 is replaced with Ala, NPM is without effect. These results provide additional evidence that the binding site for FMN is in proximity to residue Cys39. The LOV2Q43H mutant, which displays a photochemical reactivity similar to that of LOV1, also loses the majority of its chromophore in response to NPM treatment (Table 3). The effects of NPM on FMN binding to LOV1 or LOV2 suggest a structural difference between the two domains. It is likely that the folding of LOV2 differs from that of LOV1, resulting in a structure that protects Cys39 from chemical modification by NPM.

DISCUSSION

The experiments described above were aimed at characterizing the biochemical and photochemical properties of the FMN-binding domains of the plant blue light receptor, phototropin. Our results demonstrate that light sensing by phototropin is mediated by the two chromophore binding domains of the flavoprotein photoreceptor and suggest that the photoexcitation mechanism occurs via the formation of a FMN−cysteinyl adduct.

Association of FMN with the LOV Domains of Phototropin. The two FMN-binding domains of phototropin, designated LOV1 and LOV2, exhibit absorption spectra that are very similar to the action spectrum for phototropism (Figure 1A; *12*). Similar spectral properties were also observed for the full-length phototropin protein expressed in cultured insect cells (*8*). Such characteristics are typical of flavin compounds dissolved in apolar solvents (*30*), suggesting that the FMN chromophore bound to LOV1 and LOV2 is constrained within a restricted hydrophobic environment. Indeed, the FMN moiety is tightly associated with each of the LOV domain apoproteins (*12*) and is released only upon denaturation (Figure 1B).

The LOV domains belong to the PAS domain superfamily and function as internal redox sensors for a wide range of proteins (*11*). Crystal structures of three PAS domains have recently been determined and include those from the FixL protein from *Bradyrhizobium japonicum* (*31*), the human HERG potassium channel (*27*), and photoactive yellow protein (PYP) (*26*, *28*). Each of these structures has been shown to enclose a core region within the protein. In the case of the FixL and PYP PAS domains, this core site is associated with the binding of a prosthetic group (*32*, *33*). Sequence alignment analysis of more than 300 PAS domains indicates that they all contain the basic secondary structure elements that are found in PYP: the PAS core, the helical connector, and the β-scaffold structural elements (*11*). Therefore, PAS domains appear to share a striking degree of structural similarity despite exhibiting diverse functional roles.

As for the HERG, the FixL, and PYP PAS domains, the predicted three-dimensional structures of LOV1 and LOV2 were also found to enclose a central pocket that could function as a potential binding site for FMN (Figure 5A). The effects of site-directed mutagenesis on selected amino acid residues located within or nearby the central cavity (Figure 5B,C) of LOV1 and LOV2 demonstrate the importance of this region in FMN binding. Replacement of the aromatic side chain of Phe23 with Tyr (F23Y) resulted in a complete loss of chromophore binding for LOV1 and a dramatic reduction (70%) in the level of FMN binding for LOV2 (Table 2). Sequence alignment analysis indicates that Phe23 is highly conserved in all phototropin and phototropin-like proteins (Figure 4) and is located within the PAS core segment. The F23Y substitution effect on FMN binding to LOV1 and LOV2 is therefore consistent with an involvement of the PAS core in cofactor binding. Ser20 is also situated within the predicted PAS core of LOV1 and LOV2. Replacement of Ser20 with Phe caused a dramatic effect on FMN binding in both LOV domains of phototropin (Table 2). The S20F substitution corresponds to a point mutation found in the LOV domain of WC-1, a putative blue light photoreceptor from *N. crassa* (*29*), a mutation that produces a phenotype blind to blue light. Thus, it is possible that the blind phenotype observed in the mutants of *Neurospora* results from a lack of chromophore binding to WC-1.

Whether the LOV domain of WC-1 binds a blue light-sensing chromophore, let alone a flavin, remains to be determined.

Asn38, Arg40, and Gln43 are part of the conserved motif GRNCRFLQ, also located within the PAS core of LOV1 and LOV2 (Figure 4). The single-amino acid exchanges N38D, R40D, and Q43H in LOV1 or LOV2 resulted in a loss or reduction of FMN binding (Table 2). Although these data support the involvement of the PAS core in cofactor binding, further analysis is required to establish whether these mutations have a direct or indirect effect on FMN binding by LOV1 and LOV2. Studies are now underway to determine the crystal structures of the phototropin LOV domains.

The slightly divergent absorption spectra of LOV1 and LOV2, together with their different extinction coefficients, indicate a difference between the chromophore microenvironments of each domain. The effects of NPM on FMN binding (Table 3) also indicate a structural difference between the LOV1 and LOV2 domains. Treatment of LOV1 with NPM results in a release of chromophore, indicating that the flavin-binding site of LOV1 is accessible to this thiol reagent. Site-directed mutagenesis of LOV1 demonstrates that the target site of chemical modication by NPM is not Cys66 but residue Cys39, which belongs to the conserved motif GRNCRFLQ situated within the PAS core. This observation provides further support for a role of the PAS core in cofactor binding and is consistent with earlier biochemical studies demonstrating an involvement of a thiol group in the light-dependent phosphorylation of phototropin (*34*). No effect of NPM on FMN binding was observed for LOV2, suggesting that the flavin-binding site for this domain is not accessible to NPM. Determination of the three-dimensional structures for LOV1 and LOV2 will help test this hypothesis.

LOV Domains of Phototropin Function as Light Sensors. Under aerobic conditions, illumination of LOV1 or LOV2 with white light, UV-A/blue light, or blue light resulted in the formation of a species that exhibits a single absorption maximum at 380 nm in the spectral region between 300 and 550 nm (Figure 2). For both LOV domains, the absorption spectrum of the final photoproduct is very similar to that previously assigned to flavin C(4a)−thiol adducts (*16*). The light-induced fluorescence decay observed for LOV1 and LOV2 (Figure 1B) also corresponds with the nonfluorescent properties of a thiol adduct species (*16*; V. Massey, personal communication). Replacement of Cys39 with Ala in both LOV domains abolishes the photobleaching reaction (Figure 6), strongly supporting the hypothesis that phototropin photoactivation occurs via the formation of a flavin−thiol adduct. Further studies are now required to determine whether the light-induced formation of the FMN−cysteinyl adduct occurs at the C(4a) position of the flavin isoalloxazine ring.

CD spectral analysis in the visible region provides additional information regarding alterations within the chromophore environment of the phototropin LOV domains upon illumination. The light-induced visible CD changes observed for LOV2 (Figure 7) most likely reflect a considerable alteration in the FMN microenvironment in response to high-intensity white light irradiation. These changes were undetectable with the C39A mutant, again suggesting that the alteration in the chromophore environment results from the formation of the FMN−Cys39 adduct.

The light-induced formation of the postulated flavin−cysteinyl adduct was found to be fully reversible in the absence of light (Figure 3). Thus, the LOV domains of phototropin appear to undergo a self-contained photocycle as it is the case for the bacterial blue light receptor, PYP (*26*). The rate of photoproduct formation and regeneration for LOV1 and LOV2 appeared to follow first-order kinetics, suggesting that no additional reactant, other than FMN, is involved in the photoreaction cycle (Figure 3). The rate of dark regeneration for each LOV domain was reduced by approximately 7-fold when studied on ice (Table 1). The slower dark regeneration at lower temperatures may be attributed to the nature of the reverse reaction that would require breaking of the proposed covalent linkage between the FMN chromophore and the thiol group of residue Cys39. The rate constants determined for dark regeneration (k_{reg}), either at room temperature or on ice, indicate that the regeneration process occurs more rapidly for LOV1 (Table 1). The rate of photoproduct formation for either domain was unaffected at lower temperatures but depended solely on light quality and quantity. High-intensity white light (45 000 μmol m^{-2} s^{-1}) and monochromatic blue light (55 μmol m^{-2} s^{-1}) were equally effective in driving photoproduct formation (Table 1), whereas illumination with red light (5000 μmol m^{-2} s^{-1}) was without effect (data not shown).

LOV1 and LOV2 Exhibit Differential Light Sensitivity. While our data suggest that the photochemistry of LOV1 and LOV2 involves the formation of a FMN-Cys39 adduct, LOV1 appears to be less photosensitive than LOV2. The relative quantum efficiencies measured under broad-band blue light were 0.045 for LOV1 and 0.44 for LOV2, a more than 10-fold difference. Since the rate of dark regeneration is more than 2 times as fast for LOV1 (half-lives of 78 and 201 s on ice for LOV1 and LOV2, respectively), the equilibrium level of LOV1, under illumination conditions whereby steady-state concentrations of photobleaching and regeneration are reached, will be far lower than that of LOV2. Under these conditions, the equilibrium constants (K_{eq}) for LOV1 and LOV2 are 1.12 (0.01/0.0089) and 31 (0.106/0.0034), respectively, a 27-fold difference. Thus, even in the experiment illustrated in Figure 2 where high-intensity white light was used, under steady-state conditions, 40% of LOV1 exists in the unreacted form whereas white light drove the LOV2 bleaching reaction to completion. Whether these differences are reflected by the properties of the LOV domains in the full-length protein remains to be determined.

The differential light sensitivity of LOV1 and LOV2 is also reflected in the degree of chromophore fluorescence quenching exhibited by the two domains. Therefore, in agreement with the relative photochemical efficiencies of the phototropin LOV domains, LOV2 exhibits a higher degree of fluorescence quenching than LOV1 (Figure 1B). The extent of fluorescence quenching of the protein-bound chromophore was reduced in both C39A mutants of LOV1 and LOV2 (Figure 6C). However, the effect was far more dramatic for the C39A mutant of LOV2. The difference in fluorescence quenching reflects, in part, the fact that the light energy absorbed by either LOV1C39A or LOV2C39A is no longer consumed by photochemistry and is therefore released as fluorescence. The more dramatic effect observed for LOV2C39A is consistent with the greater photochemical efficiency of LOV2. However, the differences in quantum

efficiencies between LOV1 and LOV2 do not provide a complete explanation for the fluorescence properties of LOV1C39A and LOV2C39A. It is likely that the chromophore microenvironment of LOV2C39A is such that the fluorescence yield is far higher than that of the released chromophore, whereas no such amplification effect is observed with LOV1C39A. Whether LOV1 and LOV2 exhibit different light sensing roles within the native phototropin protein will require further investigation.

To our knowledge, the photochemical reaction mechanism observed for LOV1 and LOV2 is unique among those known for flavoproteins. A similar light-dependent reaction was found for the LOV2 domain of PHY3 (data not shown), suggesting that the mechanism is shared between all phototropin and phototropin-like proteins. Our results therefore demonstrate that the initial photoexcitation mechanisms of phototropin most likely involve the formation of a FMN−cysteinyl adduct within the LOV domain apoproteins, leading to a dramatic alteration in chromophore conformation. We hypothesize that the light-driven reaction results in conformational changes of the phototropin LOV domains, which in turn leads to the activation of the receptor kinase and the initiation of the phototropic signaling.

ACKNOWLEDGMENT

We thank Vincent Massey, Pill-Soon Song, and Wolfhart Rüdiger for critical reading of the manuscript.

REFERENCES

1. Briggs, W. R., and Huala, E. (1999) *Annu. Rev. Cell Dev. Biol. 15*, 33−61.
2. Ahmad, M., and Cashmore, A. R. (1993) *Nature 366*, 162−166.
3. Lin, C., Ahmad, M., Chan, J., and Cashmore, A. R. (1996) *Plant Physiol. 110*, 1047.
4. Hoffmann, P. D., Batschauer, A., and Hays, J. B. (1996) *Mol. Gen. Genet. 253*, 259−265.
5. Huala, E., Oeller, P. W., Liscum, E., Han, I.-S., Larsen, E., and Briggs, W. R. (1997) *Science 278*, 2120−2123.
6. Frechilla, S., Zhu, J., Talbott, L. D., and Zeiger, E. (1999) *Plant Cell Physiol. 40*, 949−954.
7. Lasceve, G., Leymarie, J., Olney, M. A., Liscum, E., Christie, J. M., Vavasseur, A., and Briggs, W. R. (1999) *Plant Physiol. 120*, 605−614.
8. Christie, J. M., Reymond, P., Powell, G. K., Bernasconi, P., Raibekas, A. A., Liscum, E., and Briggs, W. R. (1998) *Science 282*, 1698−1701.
9. Ahmad, M., Jarillo, J. A., Smirnova, O., and Cashmore, A. R. (1998) *Nature 392*, 720−723.
10. Zhulin, I. B., and Taylor, B. L. (1997) *Trends Biochem. Sci. 22*, 331−333.
11. Taylor, B. L., and Zhulin, I. B. (1999) *Microbiol. Mol. Biol. Rev. 63*, 479−506.
12. Christie, J. M., Salomon, M., Nozue, K., Wada, M., and Briggs, W. R. (1999) *Proc. Natl. Acad. Sci. U.S.A. 96*, 8779−8783.
13. Massey, V., Stankovich, M., and Hemmerich, P. (1978) *Biochemistry 17*, 1−8.
14. Massey, V., and Hemmerich, P. (1978) *Biochemistry 17*, 9−16.
15. Lin, C., Robertson, D. E., Ahmad, M., Raibekas, A. A., Jorns, M. S., Dutton, P. L., and Cashmore, A. R. (1995) *Science 269*, 968−970.
16. Miller, S. M., Massey, V., Ballou, D., Williams, C. H., Jr., Distefano, M. D., Moore, M. J., and Walsh, C. T. (1990) *Biochemistry 29*, 2831−2841.
17. Thorpe, C., and Williams, C. H., Jr. (1976) *J. Biol. Chem. 251*, 7726−7728.
18. Thorpe, C., and Williams, C. H., Jr. (1981) *Biochemistry 20*, 1507−1513.
19. O'Donnel, M. J., and Williams, C. H., Jr. (1984) *J. Biol. Chem. 259*, 2243−2251.
20. Zacherl, M., Huala, E., Rüdiger, W., Briggs, W. R., and Salomon, M. (1998) *Plant Physiol. 116*, 869.
21. Nozue, K., Kanegae, T., Imaizumi, T., Fukada, S., Okamoto, H., Yeh, K.-C., Lagarias, J. C., and Wada, M. (1998) *Proc. Natl. Acad. Sci. U.S.A. 95*, 15826−15830.
22. Jarillo, J. A., Ahmad, M., and Cashmore, A. R. (1998) *Plant Physiol. 117*, 719.
23. Peitsch, M. C. (1995) *Bio/Technology 13*, 658−660.
24. Peitsch, M. C. (1996) *Biochem. Soc. Trans. 24*, 274−279.
25. Guex, N., and Peitsch, M. C. (1997) *Electrophoresis 18*, 2714−2723.
26. Genick, U. K., Borgstahl, G. E. O., Ng, K., Ren, Z., Pradervand, C., Burke, P. M., Srajer, V., Teng, T.-Y., Schidkamp, W., McRee, D. E., Moffat, K., and Getzoff, E. D. (1997) *Science 275*, 1471−1475.
27. Cabral, J. H. M., Lee, A., Cohen, S. L., Chait, B. T., Li, M., and Mackinnon, R. (1998) *Cell 95*, 649−655.
28. Pellequer, J.-L., Wager-Smith, K. A., Kay, S. A., and Getzoff, E. D. *Proc. Natl. Acad. Sci. U.S.A. 95*, 5884−5890.
29. Ballario, P., Talora, C., Galli, D., Linden, H., and Macino, G. (1998) *Mol. Microbiol. 29*, 719−729.
30. Schmidt, W. (1980) in *The Blue Light Syndrome* (Senger, H., Ed.) pp 212−220, Springer-Verlag, Berlin.
31. Gong, W., Hao, B., Mansy, S. S., Gonzalez, G., Gilles-Gonzalez, M. A., and Chan, M. K. (1998) *Proc. Natl. Acad. Sci. U.S.A. 95*, 15177−15182.
32. Baca, M., Borgstahl, G. E. O., Boissinot, M., Burke, P. M., Williams, D. R., Slater, K. A., and Getzoff, E. D. (1994) *Biochemistry 33*, 14369−14377.
33. Monson, E. K., Ditta, G. S., and Helinski, D. R. (1995) *J. Biol. Chem. 270*, 5243−5250.
34. Rüdiger, W., and Briggs, W. R. (1995) *Z. Naturforsch. 50c*, 231−234.

BI000585+